HHS Public Access

Author manuscript

Cancer Res. Author manuscript; available in PMC 2017 April 15.

Published in final edited form as:

Cancer Res. 2016 April 15; 76(8): 2206–2218. doi:10.1158/0008-5472.CAN-15-1046.

Mutant p53 promotes epithelial ovarian cancer by regulating tumor differentiation, metastasis, and responsiveness to steroid hormones

Yi A Ren[1], **Lisa K Mullany**[1], **Zhilin Liu**[1], **Alan J Herron**[2], **Kwong-Kwok Wong**[3,*], and **JoAnne S Richards**[1,*]

[1]Department of Molecular and Cellular Biology, Baylor College of Medicine, Houston, TX 77030, USA

[2]Department of Pathology & Immunology, Baylor College of Medicine, Houston, TX 77030, USA

[3]Department of Gynecologic Oncology and Reproductive Medicine, The University of Texas MD Anderson Cancer Center, Houston, TX 77030, USA

Abstract

Mutations in the tumor protein p53 (TP53) are the most frequently occurring genetic events in high-grade ovarian cancers, especially the prevalence of the TP53R175H mutant allele. In this study, we investigated the impact of the TP53R175H mutant allele on epithelial ovarian cancer (EOC) in vivo. We used the Pten/KrasG12D mutant mouse strain that develops serous EOC with 100% penetrance to introduce the mutant Trp53R172H allele (homolog for human TP53R175H). We demonstrate that the Trp53R172H mutation promoted EOC, but had differential effects on disease features and progression depending on the presence or absence of the wild-type (WT) TP53 allele. Heterozygous WT/Trp53R172H alleles facilitated invasion into the ovarian stroma, accelerated intraperitoneal metastasis, reduced TP53 transactivation activity, but retained responsiveness to nutlin-3a, an activator of WT TP53. Moreover, high levels of estrogen receptor alpha in these tumors enhanced the growth of both primary and metastatic tumors in response to estradiol. Ovarian tumors homozygous for Trp53R172H mutation were undifferentiated and highly metastatic, exhibited minimal TP53 transactivation activity, and expressed genes with potential regulatory functions in EOC development. Notably, heterozygous WT/Trp53R172H mice also presented mucinous cystadenocarcinomas at 12 weeks of age, recapitulating human mucinous ovarian tumors, which also exhibit heterozygous TP53 mutations (~50–60%) and KRAS mutations. Therefore, we present the first mouse model of mucinous tumor formation from ovarian cells and supporting evidence that mutant TP53 is a key regulator of EOC progression, differentiation, and responsiveness to steroid hormones.

*Corresponding authors to whom requests can be sent: JoAnne S. Richards, Ph.D., Professor, Department of Molecular and Cellular Biology, Baylor College of Medicine, Mail Stop 130, One Baylor Plaza, Houston, TX 77030, USA, Phone: 713.798.6238, Fax: 713.790.1275, ; Email: joanner@bcm.edu. Kwong-Kwok Wong, Ph.D., Professor, Department of Gynecologic Oncology and Reproductive Medicine, University of Texas M.D. Anderson Cancer Center, Houston, TX 77030, USA, Phone: 713.792.0229, ; Email: kkwong@mdanderson.org.

The authors do not have any conflicts of interest to disclose.

Author Contributions

Y.A.R. and J.S.R. provided the conception and design for the studies. Y.A.R., L.K.M., and K.K.W. developed methodology. Z.L. analyzed the microarray data. A.J.H. provided pathological diagnosis. Y.A.R. performed all experiments and acquisition of data.

Keywords

mutant p53; epithelial ovarian cancer; mucinous; differentiation; steroid hormone

Introduction

As the fifth leading cause of death in women, ovarian cancer is a devastating disease without effective detection and therapeutic management. The majority (>90%) of human ovarian cancers are of epithelial cell origin (1,2) and based on their histological features are categorized as serous, endometrioid, mucinous and clear cell type (3). These subtypes differ significantly in their potential sites of origin, molecular signature, prognosis and response to treatments, making epithelial ovarian cancer (EOC) not a single disease, but multiple diseases (4).

Mutations in the tumor protein TP53 (P53) are among the most common and frequent events in EOC, especially in the high-grade serous subtype (>90%) (The Cancer Genome Atlas Research Network, TCGA) (5). Furthermore, the R175H mutation of *TP53* is one of the most frequently occurring (3.8%) in serous EOC (TCGA) (6). When the $Trp53^{R172H}$ mutation (mouse homolog for the R175H mutation in human) is expressed in cells depleted of *Apc* and *Pten*, or in cells with inactivated *Rb* and *Brca1/2*, it promotes epithelial ovarian tumor progression and metastasis (7,8). Moreover, a recent examination of TCGA database reveals that p53 gain-of-function (GOF) mutations, including the R175H mutation, in ovarian tumors of human patients are associated with a higher incidence of platinum resistance, local recurrence, and distant metastasis (9). Intriguingly and importantly, recently published studies show that *TP53* mutations in human EOC tumor samples are frequently present as heterozygous (10) (and Mullany *et al.*, *Neoplasia*, in press), indicating that it is critical to understand not only the biology of tumors homozygous for wild-type or mutant alleles of p53, but also the interaction between wild-type and mutant alleles in a tumor type-specific context.

Oncogenic alterations are necessary for ovarian cancer development, but strong evidence indicates that steroid hormones such as estradiol also play critical roles in promoting the timing of onset, progression and metastasis of EOC (11–13). The majority of EOC cases occur during the peri- and post-menopausal period (peak at ages 65–75), when the tumor-promoting effects of estradiol are unopposed by progesterone (1). Several recent epidemiological and clinical studies suggest that the expression of steroid hormone receptors is linked to ovarian cancer subtypes, progression, prognosis and response to hormone treatment (14–18). Thus, how oncogenic factors, TP53 and steroid hormones interact to impact EOC development is becoming an emerging area of research that is highly relevant for developing and revising clinical therapeutic strategies.

Our laboratory previously generated mice in which the *Pten* gene was conditionally deleted and $Kras^{G12D}$ was activated by Cre-recombinase driven by *Amhr2* promoter (*Pten/Kras* mutant mice) (19,20). These mice developed ovarian surface epithelial (OSE) cell derived, low-grade serous adenocarcinomas with 100% penetrance. When *Trp53* was deleted in the OSE cells of the *Pten/Kras* mutant mice, tumor growth was markedly reduced but the

expression of estrogen receptor alpha was elevated (21), and when exposed to estradiol, the primary ovarian lesions grew rapidly and metastasized throughout the intraperitoneal cavity. These studies documented clearly and for the first time that the functional status of TRP53 can determine steroid hormone responsiveness in EOC cells.

Based on the foregoing considerations, we hypothesized that 1) specific *Trp53* mutations would not only alter tumor growth and metastasis but also the responsiveness of EOC cells to steroid hormones, 2) the effect of any given mutation would also depend on whether a WT allele was present or absent, and 3) each condition would exhibit a distinct molecular signature. Specifically, because the human $TP53^{R175H}$ allele is frequently associated with high-grade ovarian cancer, we introduced a germ-line *Trp53* R172H mutant allele into our *Pten/Kras* strain to generate OSE cells either heterozygous or homozygous for the $Trp53^{R172H}$ mutant allele. Our findings indicate that expression of heterozygous *Trp53* mutant alleles drives a tumor phenotype that is distinct from that of WT *Trp53* or homozygous *Trp53* mutant alleles in determining ovarian tumor behavior and outcome.

Materials and Methods

Animal Studies

All animals were housed under a 14-hour light/10-hour dark schedule in the Center for Comparative Medicine at Baylor College of Medicine and provided food and water *ad libitum*. All animals were maintained according to the National Institutes of Health (NIH) Guide for the Care and Use of Laboratory Animals and approved by the Animal Care and Use Committee at Baylor college of Medicine. Mice carrying the germline $Trp53^{R172H}$ mutation were generated by Dr. Guillermina Lozano (MD Anderson Cancer Center, Houston, Texas) (22). These mice were bred to $Pten^{f/f};Kras^{G12D};Amhr2\text{-}Cre$ *(PK)* mice described previously to obtain *PK* mice expressing WT *Trp53* ($PKP53^{+/+}$), and either heterozygous ($PKP53^{H/+}$) or homozygous mutant $Trp53^{R172H}$ ($PKP53^{H/H}$) (19).

Laser capture microdissection and sequencing of human mucinous tumor samples

Laser capture microdissection of human mucinous tumor samples is described in detail in supplemental materials. DNA was extracted from microdissected tumor cells using a QIAamp DNA Micro Kit (Qiagen, Valencia, CA) and quantified using a NanoDrop spectrometer (NanoDrop, Rockland, DE). Mutation analysis of TP53 (Exons 5–8) was performed by Sanger Sequencing using PCR primers as described previously (23).

Injection of tumor cells into syngenic mice and hormone pellet implants

Isolation, culturing, and injection of OSE cells from genetically engineered mice are described in detail in Supplementary Materials and Methods. Genotype-confirmed mice of WT and mutant *Trp53* status were implanted with one-half of a 0.36-mg estradiol pellet (0.36 mg) or with progesterone pellet (25 mg) one day prior to giving estradiol pellet (SE-121 for 17β-estradiol and P-131 for progesterone, Innovative Research of America, Sarasota, FL), and tumor progression was monitored at 1, 2 or 4 weeks after pellet implanting.

RNA extraction, real-time RT-PCR and microarray analyses

DNA expression vectors (0.20 μg DNA ; empty vector or vector expressing mutant R175H *TP53*) were transfected into cells using Attractene Transfection Reagent (Qiagen, Valencia, CA) according to the manufacturer's protocol, and lysed for RNA extraction 24 hours following transfection. Total RNA extraction, reverse transcription, real-time PCR and microarray analyses were described in Supplementary Materials and Methods. The microarray data have been deposited to GEO with the accession number GSE65206.

Cell adhesion, proliferation and viability assays

To assess cell attachment to the culture dish, $PKP53^{+/+}$, $PKP53^{H/+}$ and $PKP53^{H/H}$ OSE cells at similar passages were plated at 100,000 cells/well in a 12-well plate. After culturing for 2 hours, the plates were gently swirled and pipetted three times. Unattached cells were removed; attached cells that remained on the dish were trypsinized and counted with a hemocytometer. To measure the rate of proliferation, OSE cells at similar passages were plated at 100,000 cells/well in each 12-well plate. After 36 hours of culture, when cells of all genotypes have attached well and are proliferating but not confluent, cells were trypsinized and counted using a hemocytometer. Cell viability was measured using the WST-1 assay according to manufacturer's instruction following 72 hours of nutlin-3a treatment. The WST-1 reagent was incubated with the cells for 4 hours before its absorbance was read at 450 nm (Roche, Pleasanton, CA).

Western blot analyses

Whole cell lysate were collected using methods previous described (24). Proteins were separated using a 10% Bis-Tris gel and transferred to an immobilon-P membrane (Millipore). Primary antibodies used included ESR1 (sc-542) (1:1000), PR (sc-7208) (1:1000), and p53 (sc-6243) (1:1000) (Santa Cruz Biotechnology) and signals were detected using the Peirce ECL 2 Western Blotting Substrate (Thermo Scientific).

TP53 luciferase assay

OSE cells were transfected according to manufacturer's instruction (P53 Cignal Reporter Assay Kit, Qiagen Sciences). Nutlin-3a (generously provided by Dr. Robert Bast, MD Anderson Cancer Center, Houston, TX) or DMSO vehicle control were added to the cultures after overnight transfection and luciferase assays were performed after 24 hours of treatment using the Dual-Glo Luciferase Assay System (Promega).

Statistical analysis

Data are represented as mean ± SEM. Comparisons between experimental groups with a single variance were analyzed using unpaired Student's *t*-test, and a two-tailed $p<0.05$ was considered statistical significance. Comparison between experimental groups with more than one variances were analyzed using randomized two-way ANOVA. When ANOVA indicated overall significance, Student-Newman-Keuls test was used to compare individual means.

Results

Trp53 R172H mutation promotes epithelial ovarian tumor progression

Before 12 weeks of age, ovarian epithelial tumors in the $PKP53^{+/+}$ and $PKP53^{H/+}$ mice exhibited similar serous, papillary-like structures on the surface of the ovary that stained positively for cytokeratin 8 (KRT8), a marker for OSE cells (Fig. 1A). However, the tumors in the $PKP53^{H/+}$ mice appeared more locally invasive into the ovarian stroma and more metastatic to the omentum than those in the $PKP53^{+/+}$ mice of the same age (Fig. 1A). Furthermore, the $PKP53^{H/+}$ mice died consistently between 12 and13 weeks of age (n=8), whereas most $PKP53^{+/+}$ mice died between 16 and 40 weeks of age (Fig. 1B and 1C) (19), indicative of a more aggressive tumor phenotype in the $PKP53^{H/+}$ mice (Fig. 1B). Interestingly and unexpectedly, 80% $PKP53^{H/+}$ mice also developed mucinous-like tumors between 8 and 12 weeks of age, as described below in Figure 3.

Epithelial ovarian tumor expressing homozygous *Trp53*^{R172H} mutation have early onset transformation and metastasis

Papillary-like epithelial ovarian lesions also developed in homozygous $PKP53^{H/H}$ mice as early as 4 weeks of age and appeared to be in a more advanced stage compared to those in $PKP53^{H/+}$ mice of the same age (Fig. 2A, upper panels, red arrows). Notably, a significant number of KRT8-positive metastatic tumor cells were present on the omentum of $PKP53^{H/H}$ mice at 4 weeks of age, while only minimal metastasis to the omentum was observed in $PKP53^{H/+}$ mice (Fig. 2A, lower panels of KRT8 staining). The $PKP53^{H/H}$ tumor cells that metastasized to the omentum were highly proliferative as shown by KRT8 and phospho-histone H3 (p-HH3) co-staining (Fig. 2A, lower panels). Unfortunately, the $PKP53^{H/H}$ mice died rapidly at 5 weeks from as yet unknown causes (Fig 1B and 1C).

To further investigate the behavior of $PKP53^{H/H}$ OSE cells *in vivo*, we generated OSE cell lines from $PKP53^{H/H}$ mice and injected these cells into the ovaries of syngenic hosts. Within 2 weeks, large, undifferentiated tumors were rampant in the ovaries injected with $PKP53^{H/H}$ cells (Fig. 2B, upper panels). Consistent with metastatic tumors seen in $PKP53^{H/H}$ mice, these injected tumor cells also grew rapidly at sites throughout the intraperitoneal cavity such as the bowel mesentery, the pancreas and the omentum (Fig. 2B, lower panels). In the pancreas, these tumor cells appeared invasive.

OSE tumors expressing heterozygous *Trp53*^{R172H} develop mucinous-like structures

A unique feature of the $PKP53^{H/+}$ mice is that they developed large cystic-like structures within the ovary between 8 and 12 weeks of age (8/10 females) (Fig. 1B and Fig. 3A, upper panels); these structures contained serous as well as mucinous-, secretory- like cells that were not observed in $PKP53^{+/+}$ or $PKP53^{H/H}$ mice at any age, and morphologically they resemble mucinous ovarian EOC in human patients (Fig. 3B, upper panel). KRT8 and H&E staining showed that the $PKP53^{H/+}$ OSE cells (red arrows) invaded the ovarian stroma and presented various stages of differentiation into secretory mucinous-like structures (Fig. 3A, lower panels, black arrows). A previously characterized human ovarian cancer cell line (RMUG-L) that was obtained from a human mucinous ovarian carcinoma, carries heterozygous WT and mutant *TP53* (c.614A>G) alleles as confirmed by us recently (23),

exhibited a similar morphological and secretory phenotype when innoculated into the intraperitoneal cavity of the severely compromised immunodeficient (SCID) mice (Fig. 3C) (25,26). To confirm the mucinous tumor phenotype in the *PKP53*$^{H/+}$ ovary, we performed immunohistochemical analyses using an antibody detecting Mucin 5AC (MUC5AC), a marker of the human ovarian mucinous-like cancer subtype (Fig. 3D) (27,28). Indeed, the secretory structures in the mouse tumors are immuno-positive for MUC5AC (Fig. 3C) and KRT8 (Fig. 3E), but not immuno-positive for FOXL2 (a marker for granulosa cells) or PAX8 (a marker for Fallopian tube secretory cells) (Fig. 3E) (29,30), suggesting that mucinous-like cells may arise from the ovarian surface epithelial cells and not from granulosa cells or Fallopian tube epithelial cells. In some cystic structures, mucinous cells that were KRT8 and MUC5AC positive were contiguous with KRT8 positive and MUC5AC negative cells, providing further evidence that MUC5AC-positive secretory cells and KRT8-positive epithelial cells may share a common precursor (Fig. 3F).

To determine the mutant status of *TP53* in human mucinous EOCs, we have sequenced laser capture microdissected mucinous tumor cells from 12 human patient samples. Of these, four samples (33%) had mutations in exons 5–8 of the *TP53* gene, and in all 4 cases, the wild-type allele is still expressed (Fig. 3B, lower panel; and Supplemental Fig. 1). These results support recent studies indicating that a significant number of human mucinous tumors express heterozygous mutant and wild type alleles, including the R175H mutation (Supplemental Table 1) (10,31). Specifically, supplemental data provided in the study by Mackenzie *et al.* (10) show that in a dataset composed of 37 laser capture microdissected human mucinous ovarian tumor samples, 63% had mutations in *KRAS*, 56.8% had mutations in *TP53*, and 36% of tumors with *KRAS* mutations also had mutations in *TP53.* Importantly, 68% of *TP53* mutations in these patient samples are heterozygous, with the co-existence of a wild type and mutant allele. This observation is also consistent with the studies by Rechsteiner *et al.* (31), which demonstrated that at least half (57%) of human mucinous ovarian tumor samples express mutations in *KRAS*, and 37% of these mutations are co-expressed with mutations in *TP53*. To our knowledge, the *PKP53*$^{H/+}$ mutant mouse strain is the first model that presents a mucinous-like tumor phenotype that is not derived from cells of the Müllerian duct or gut (2,32).

Epithelial ovarian tumors expressing heterozygous *Trp53*^{R172H} have elevated expression of estrogen receptor alpha

To determine how expression of the *Trp53*^{R172H} mutant allele affects OSE tumor responses to steroid hormones, we examined the expression and localization of estrogen receptor alpha (ESR1) and progesterone receptor (PR) in tumor cells of *PKP53*$^{+/+}$, *PKP53*$^{H/+}$ and *PKP53*$^{H/H}$ mice using *in vivo* and *in vitro* approaches. At 8 weeks of age (Fig. 4A and Supplemental Fig. 2), the majority of *in vivo* ovarian tumor cells positive for KRT8 in the *PKP53*$^{+/+}$ mice were not ESR1-positive, whereas the majority of the KRT8-positive tumor cells in *PKP53*$^{H/+}$ mice exhibited intense ESR1 staining. KRT8-positive tumor cells in the *PKP53*$^{H/H}$ mice exhibited low ESR1 staining. Consistent with these observations, the levels of *Esr1* and *Pgr* mRNA are elevated in the *PKP53*$^{H/+}$ tumor cells compared to those of the other two genotypes, and this difference was statistically different for *Esr1* but not *Pgr* (Fig. 4B). ESR1 protein levels were also analyzed in cell lines derived from OSE cells isolated

from ovaries of mice of each genotype. Western blotting confirmed that ESR1 was elevated in cells derived from the *PKP53*$^{H/+}$ mice compared to the other two genotypes. Western blots for PR indicated that the protein levels of the PR-A isoform were higher than those of the PR-B isoform in cells of all three genotypes, and that PR-A was higher in *PKP53*$^{+/+}$ cells compared to the other two (Fig. 4C). When OSE cells were treated with nutlin-3a, a small molecule that stabilizes active TRP53 protein, it increased *Esr1* mRNA expression in *PKP53*$^{+/+}$ and *PKP53*$^{H/+}$ cells, but not in *PKP53*$^{H/H}$ cells (Fig. 4D), suggesting that TRP53 regulates transcription of *Esr1* gene in OSE cells, and the presence of both the wild type *Trp53* and mutant R172H alleles has the strongest inductive effect. These results support several previous studies that have shown direct transcriptional regulation of *ESR1* by wild-type p53 using chromatin immunoprecipitation (ChIP) analyses (33,34). Under normal physiological conditions, wild type TP53 is expressed at very low levels in most cells. However, it has been shown that the expression of wild type TP53 protein increases to a very high level in the presence of mutant p53 protein (35). Thus, we speculate that the presence of heterozygous TRP53 alleles in our mouse ovarian tumor cells, as well as in relevant human tumors, elevates expression of ESR1 through wild-type p53 stabilization. In contrast to *Esr1*, nutlin-3a did not increase *Pgr* mRNA expression in any of the three cell lines (Fig. 4D). When a vector expressing the mutant R175H allele was transfected into *PKP53*$^{+/+}$ cells, it induced increased expression of *Esr1* but not *Pgr* mRNA (Fig. 4E), also suggesting that co-expression of wild type *Trp53* and the mutant R175H alleles enhances transcription induction of the *Esr1* gene. Interestingly, while many adjacent KRT8-positive epithelial tumor cells express high levels of ESR1, ESR1 expression is not present in the differentiated, secretory mucinous type tumor (Fig. 4F). This observation is consistent with variable ESR1 expression in human mucinous ovarian tumors (36), and suggests that ESR1 may be present and play a role during early stages of mucinous ovarian tumor development.

Estradiol promotes tumor growth on the ovary and omentum in *PKP53*$^{H/+}$ mice

Based on the elevated expression of *Esr1* mRNA and protein in tumors of the *PKP53*$^{H/+}$ mice, we next investigated the *in vivo* response of tumors in these mice to estradiol. Four weeks of estradiol exposure induced rampant growth and local invasion of the primary tumors within the ovarian stroma and proliferation of metastatic cells present on the omentum (Figure 5A and 5B). We also tested the effect of estradiol on *PKP53*$^{H/+}$ tumor cells by subcutaneously injected these cells into ovariectomized syngenic hosts (Figure 5E). Estradiol significantly stimulated subcutaneous tumor growth of the *PKP53*$^{H/+}$ tumor cells. Previously we have demonstrated that progesterone blocks effects of estradiol on tumor growth and metastasis in the *PKP53*$^{-/-}$ mice (11). However, when progesterone was given one day before estradiol to the *PKP53*$^{H/+}$ mice, it did not block estradiol-induced tumor growth either in the primary tumor or at metastatic sites on the omentum (Figure 5C). We quantified the percentage of pHH3-positive proliferating KRT8-positive tumor cells, further confirming our observations of tumor grow rate with estradiol and progesterone treatment (Figure 5D). Thus, we conclude that estradiol promotes primary and omental metastatic tumor growth in *PKP53*$^{H/+}$ mice, and this effect is not blocked by progesterone in the context analyzed.

Expression of the *Trp53^{R172H}* mutant allele alters OSE tumor differentiation and promotes their proliferation and survival

To obtain a comprehensive understanding of the molecular events occurring in the OSE tumor cells expressing *Trp53^{R172H}*, we performed microarray analyses on RNA prepared using unpassaged OSE cells isolated from *PKP53$^{+/+}$*, *PKP53$^{H/+}$* and *PKP53$^{H/H}$* mice (Fig. 6A). Heatmap analyses showed that gene expression patterns are quite similar between *PKP53$^{+/+}$* and *PKP53$^{H/+}$* tumor cells, despite the marked differences in the responses of tumor cells to estradiol in these mice. *PKP53$^{H/H}$* cells had a markedly distinct gene expression profile compared to the other two genotypes.

To verify the gene expression profiles, real-time qPCR analyses were performed (Fig. 6B). Genes known to be associated with OSE stem cells (*Lgr5*, *Aldh1a1* and *Aldh1a7*) exhibited significantly reduced levels of mRNA in the *PKP53$^{H/H}$* tumor cells. Three epithelial cell differentiation-regulating transcription factors, *Lhx9*, *Amhr2*, and *Foxa2*, were also substantially dysregulated in these cells: *Lhx9* was undetectable, *Amhr2* was minimal and *Foxa2* was increased in the *PKP53$^{H/H}$* tumors. The expression of several secretory factors was altered: *Cxcl12* and *Bdnf* mRNAs increased in tumors of the *PKP53$^{H/H}$* mice but not in the *PKP53$^{+/+}$*, *PKP53$^{H/+}$* mice whereas *Igfbp6* mRNA was drastically decreased in these cells. Expression of apoptosis and cell survival regulators *Ddit4* and *Dapk2*, among many other apoptosis regulators, was diminished in *PKP53$^{H/H}$* cells; while cell cycle regulators, such as *Ccnb1*, were highly expressed in these cells. Lastly, several tumoriogenic regulators in OSE tumors had differentially regulated expression in the *PKP53$^{H/H}$* cells; *Ndn* was dramatically reduced whereas *Ddx39*, and *Eya4* were significantly increased. We further analyzed cell adhesion and proliferation in the *PKP53$^{+/+}$*, *PKP53$^{H/+}$* and *PKP53$^{H/H}$* cells. As shown in Fig. 6C, cell adhesion was reduced in both *PKP53$^{H/+}$* and *PKP53$^{H/H}$* cells, and the *PKP53$^{H/H}$* cells were also significantly more proliferative than cells of the other genotypes.

Trp53 R172H mutation alters TRP53 activity in OSE tumors

To determine TRP53 activity in the *PKP53$^{+/+}$*, *PKP53$^{H/+}$* and *PKP53$^{H/H}$* cells, nutlin-3a, a small molecule stabilizer and activator of TRP53, was utilized (37). Nutlin-3a stabilized TRP53 protein in cells expressing WT *Trp53* as expected (Fig. 7A) (38). Expression of the *Trp53^{R172H}* stabilized TRP53 protein with or without nutlin-3a treatment in *PKP53$^{H/+}$* and *PKP53$^{H/H}$* mutant cells. Enhanced stabilization of TRP53 protein was also demonstrated by TRP53 immunofluorescent staining (Fig. 7B). Despite the high levels of TRP53 protein, the activity of TRP53 signaling pathway was reduced and negligible, respectively, in *PKP53$^{H/+}$* and *PKP53$^{H/H}$* mutant cells, as measured by a luciferase assay containing an inducible p53-reporter, either with or without nutlin-3a treatment (Fig. 7C).

In addition, we analyzed basal and nutlin-3a induced expression or repression of known TRP53 target genes in mutant cells of each genotype (Fig. 7D). Basal levels of *Cdkn1a (P21)* and *Mdm2* were reduced in the *PKP53$^{H/+}$* and *PKP53$^{H/H}$* mutant cells compared to the *PKP53$^{+/+}$* cells. However, *Cdkn1a*, *Mdm2*, *Btg2* and *Bbc3* (*Puma*) were highly induced by nutlin-3a in both the *PKP53$^{+/+}$ and PKP53$^{H/+}$* cells but not in the *PKP53$^{H/H}$* mutant cells, indicating that the presence of one mutant allele is not sufficient to suppress the activity of the wild type allele. Likewise, expression of genes suppressed by TRP53 such as *Birc5* and

Brca1 were decreased by nutlin-3a treatment in the $PKP53^{+/+}$ *and* $PKP53^{H/+}$ cells but not in the $PKP53^{H/H}$ mutant cells. Notably, the expression of *Cdkn2a* (*P16*) was highly expressed in the $PKP53^{H/H}$ mutant cells as we have observed in *Pten/Kras* mutant cells that are null for *Trp53* (21). Interestingly, despite retained transactivation activity of the wild type TRP53 in the $PKP53^{H/+}$ cells, nutlin-3a treatment effectively caused death of $PKP53^{+/+}$ cells in a dose-dependent manner, but this effect was abolished in $PKP53^{H/+}$ and $PKP53^{H/H}$ cells (Fig. 7E), reflecting potential gain-of-function effect of the R172H allele in promoting tumor survival.

Discussion

Trp53 R172H mutation impacts ovarian cancer cell initiation and progression

The R175H mutation in the human TP53 gene is one of the most frequently occurring mutations in human EOC and, based on recent analyses, is frequently expressed with one wild type allele (10). These data raise a novel and critical question about the functional activity and impact of the mutant p53 allele in the presence or absence of the WT allele (Mullany, *et al.*, *Neoplasia*, in press). Indeed, we demonstrate herein that tumors in the $PKP53^{H/+}$ mutant mice exhibit some similarities but also some marked differences from tumors in the $PKP53^{+/+}$ mice. Like the primary tumors in the $PKP53^{+/+}$ mice, those in the $PKP53^{H/+}$ mutant mice develop extensive papillary-like structures on the ovarian surface that stain positively for KRT8 before 8 weeks of age. However, $PKP53^{H/+}$ mutant tumors 1) develop faster and are more metastatic, 2) present mucinous epithelial tumors between 8 and 12 weeks of age, 3) express higher levels of ESR1 mRNA and protein and 4) are more responsive *in vivo* to estradiol than the $PKP53^{+/+}$ cells.

In line with the tumor-promoting effects of the $Trp53^{R172H}$ allele in our mouse model of EOC, homozygous $PKP53^{H/H}$ OSE cells exhibit early lesion onset and undergo more advanced papillary transformation and prominent metastasis onto the omentum as early as 4 weeks of age (39). When we injected $PKP53^{H/H}$ tumor OSE cells into the ovaries of syngenic host mice, they grew rapidly in the ovary and intraperitoneal cavity and invaded the pancreas. Thus homozygous mutant alleles exert a potent effect on the initiation, early progression and metastasis of ovarian tumor in the same genetic background. Gene profiles of the $PKP53^{H/H}$ EOC cells further document that these cells are markedly distinct from those in the $PKP53^{+/+}$ or $PKP53^{H/+}$ mice, as discussed below.

Trp53 R172H mutation alters epithelial ovarian tumor differentiation

Particularly striking, and of high clinical relevance, was the emergence of KRT8-positive mucinous-like tumors in the $PKP53^{H/+}$ mice that invade the ovary, and present a variety of differentiation stages by 8–12 weeks of age. Thus, the $Trp53^{R172H}$ mutant allele promotes, in a subset of cells, a phenotype that is distinct from the serous, papillary-like structures that develop earlier. To our knowledge, the $PKP53^{H/+}$ mice may potentially provide the first mouse model of mucinous EOC subtype arising from OSE cells, a site far removed from the presumed cervical/gut origin of mucinous tumors in women (3). Among human patients, the mucinous subtype is considered relatively uncommon but often has worse outcomes and is more resistant to conventional chemotherapy (36,40). Tumor development in the $PKP53^{H/+}$ mice resembles features of human mucinous ovarian cancer in several aspects: 1) mutation

in *KRAS* is a notable feature of the human ovarian mucinous subtype (in ~50% cases) (10,31,41–43), 2) concurrence of *KRAS* and *TP53* mutations occurs in human mucinous ovarian cancer samples (36%) (10,31), 3) a significant number of human mucinous tumors are heterozygous for mutant TP53 allele and a wild type allele (Fig 3B and Supplemental Table 1) (10), and 4) mutations in the PI3K/PTEN pathway are also a prominent feature of human mucinous ovarian cancer (10). That OSE cells may have the potential to trans-differentiate into mucinous-like, secretory tumor cells highlights 1) the plasticity of these ovarian surface epithelial cells and 2) the importance of the interactions among p53 status, cell-of-origin and the ovarian microenvironment in determining ovarian tumor cell fate decisions.

TRP53 and steroid hormone receptor status impact tumor prognosis and responsiveness to steroid hormones

We show that tumors in the $PKP53^{H/+}$ mice express elevated levels of ESR1 *in vivo* and *in vitro*, and undergo marked proliferation in the primary tumor and at metastatic sites on the omentum in response to estradiol treatment *in vivo.* Although PGR(A and B) are present in these cells, progesterone treatment prior to estradiol does not block estradiol-induced tumor growth. These results differ from those described previously in the same mutant background (11), where estradiol potently stimulated proliferation and metastasis of *Trp53* null $PKP53^{-/-}$ tumors and these responses to estradiol were completely blocked by progesterone treatment. According to these observations, TP53 status and steroid hormone receptor status could be considered together for predicting tumor prognosis and responsiveness to steroid hormones in ovarian cancer patients.

Heterozygous state with co-expression of both wild-type and *Trp53* R172H mutation represents a distinct tumor phenotype

A number of reports indicate that the *Trp53* R172H mutation exerts dominant negative (DN) effects on the WT *Trp53* allele (44,45). However, our data indicate that this mutant has other effects on the WT allele in the $PKP53^{H/+}$ tumor cells that may be context specific. First, as mentioned above, tumor morphology appeared to be quite similar between $PKP53^{H/+}$ mice and $PKP53^{+/+}$ mice, at least until later stages of tumor development when mucinous tumors arise in the $PKP53^{H/+}$ mice. Second, whereas microarray gene expression profiles are similar (but not identical) between OSE cells of these two genotypes, they are dramatically distinct from the gene expression profiles in the $PKP53^{H/H}$ cells. Third, in the presence of the *R172H* allele, p53 signaling seems to be active based on both luciferase TRP53 activity reporter assays and induction of P53 target genes upon nutlin-3a treatment. Collectively, our data and other studies provide evidence that it is possible that some ovarian cancer patients with heterozygous mutant TP53 expression will respond to therapeutic interventions which activate WT p53 signaling (46) (and Mullany *et al.*, *Neoplasia*, in press).

The vast number of genes that exhibit increased and decreased expression in the $PKP53^{H/H}$ tumor cells compared to $PKP53^{H/+}$ and $PKP53^{+/+}$ cells suggest that the homozygous mutants exert profound changes in the molecular events controlling these cells, some of which may mediate GOF mechanisms to ensure tumor survival in the absence of wild type TRP53. The uniqueness of the gene profiles in the $PKP53^{H/H}$ tumor cells is further

supported by the fact that they are also quite distinct from those in the p53 null cells of the *Pten/Kras* background (21). One example is *Eya4*, the overexpression of which has been reported in many different cancers (47–50). In comparison to cells expressing wild-type *Trp53*, the level of *Eya4* mRNA is dramatically elevated in $PKP53^{H/H}$ cells, but reduced in *PKP53* null OSE cells (21). *Eya4* and other differentially regulated genes in OSE cells expressing homozygous R172H mutant alleles versus null *Trp53* alleles may explain the distinctly different behaviors of these two OSE tumors. In particular, while epithelial ovarian tumors in the $PKP53^{H/H}$ homozygous mice exhibit early onset and metastasis, epithelial ovarian tumors in the $PKP53^{-/-}$ homozygous mice exhibit slow growth and minimal transformation (21). Thus, the status of p53 in tumor cells impacts tumor cell behavior, growth morphology, and metastatic potential.

Supplementary Material

Refer to Web version on PubMed Central for supplementary material.

Acknowledgments

Financial support: This work is supported by NIH-CA-181808 (JSR), NIH-HD-16229 (JSR), U54-HD07945 (Project 2, JSR) of SCCPIR Specialized Cooperative Centers Program in Reproduction and Infertility Research (Bert W O'Malley, BWO), and NIH-T32-HD-1765-36 (BWO). K-K W is supported in part by grants from the National Institutes of Health, including The University of Texas MD Anderson Cancer Center Specialized Program of Research Excellence in Ovarian Cancer (P50 CA08369), CA133057, and the Blanton-Davis Ovarian Cancer Research Program.

The authors thank Dr. Markus Rechsteiner for sharing data and for their insights in personal communications. The authors also thank Dr. Victor Kostyuk for statistical analyses. This project was supported by the Integrated Microscopy Core at Baylor College of Medicine with funding from the NIH (HD007495, DK56338, and CA125123), the Dan L. Duncan Cancer Center, and the John S. Dunn Gulf Coast Consortium for Chemical Genomics. This project was also supported by the Pathology and Histology Core at Baylor College of Medicine with funding from the NIH (NCI P30-CA125123). We also thank the Genomic and RNA profiling Core at Baylor College of Medicine for performing the microarray analyses.

References

1. Romero I, Bast RC Jr. Minireview: human ovarian cancer: biology, current management, and paths to personalizing therapy. Endocrinology. 2012; 153(4):1593–602. [PubMed: 22416079]
2. Kurman RJ, Shih Ie M. Molecular pathogenesis and extraovarian origin of epithelial ovarian cancer--shifting the paradigm. Human pathology. 2011; 42(7):918–31. [PubMed: 21683865]
3. Cho KR, Shih Ie M. Ovarian cancer. Annual review of pathology. 2009; 4:287–313.
4. Schuler S, Ponnath M, Engel J, Ortmann O. Ovarian epithelial tumors and reproductive factors: a systematic review. Archives of gynecology and obstetrics. 2013; 287(6):1187–204. [PubMed: 23503972]
5. Integrated genomic analyses of ovarian carcinoma. Nature. 2011; 474(7353):609–15. [PubMed: 21720365]
6. Brachova P, Thiel KW, Leslie KK. The consequence of oncomorphic TP53 mutations in ovarian cancer. International journal of molecular sciences. 2013; 14(9):19257–75. [PubMed: 24065105]
7. Szabova L, Yin C, Bupp S, Guerin TM, Schlomer JJ, Householder DB, et al. Perturbation of Rb, p53, and Brca1 or Brca2 cooperate in inducing metastatic serous epithelial ovarian cancer. Cancer research. 2012; 72(16):4141–53. [PubMed: 22617326]
8. Wu R, Baker SJ, Hu TC, Norman KM, Fearon ER, Cho KR. Type I to type II ovarian carcinoma progression: mutant Trp53 or Pik3ca confers a more aggressive tumor phenotype in a mouse model of ovarian cancer. The American journal of pathology. 2013; 182(4):1391–9. [PubMed: 23499052]

9. Kang HJ, Chun SM, Kim KR, Sohn I, Sung CO. Clinical relevance of gain-of-function mutations of p53 in high-grade serous ovarian carcinoma. PloS one. 2013; 8(8):e72609. [PubMed: 23967324]
10. Mackenzie R, Kommoss S, Winterhoff BJ, Kipp BR, Garcia JJ, Voss J, et al. Targeted deep sequencing of mucinous ovarian tumors reveals multiple overlapping RAS-pathway activating mutations in borderline and cancerous neoplasms. BMC cancer. 2015; 15:415. [PubMed: 25986173]
11. Mullany LK, Liu Z, Wong KK, Deneke V, Ren YA, Herron A, et al. Tumor repressor protein 53 and steroid hormones provide a new paradigm for ovarian cancer metastases. Mol Endocrinol. 2014; 28(1):127–37. [PubMed: 24264574]
12. Laviolette LA, Garson K, Macdonald EA, Senterman MK, Courville K, Crane CA, et al. 17beta-estradiol accelerates tumor onset and decreases survival in a transgenic mouse model of ovarian cancer. Endocrinology. 2010; 151(3):929–38. [PubMed: 20056833]
13. Trevino LS, Giles JR, Wang W, Urick ME, Johnson PA. Gene expression profiling reveals differentially expressed genes in ovarian cancer of the hen: support for oviductal origin? Hormones & cancer. 2010; 1(4):177–86. [PubMed: 21761365]
14. De Stefano I, Zannoni GF, Prisco MG, Fagotti A, Tortorella L, Vizzielli G, et al. Cytoplasmic expression of estrogen receptor beta (ERbeta) predicts poor clinical outcome in advanced serous ovarian cancer. Gynecologic oncology. 2011; 122(3):573–9. [PubMed: 21665249]
15. Zhao D, Zhang F, Zhang W, He J, Zhao Y, Sun J. Prognostic role of hormone receptors in ovarian cancer: a systematic review and meta-analysis. International journal of gynecological cancer : official journal of the International Gynecological Cancer Society. 2013; 23(1):25–33. [PubMed: 23221605]
16. Sieh W, Köbel M, Longacre TA, Bowtell DD, deFazio A, Goodman MT, et al. Hormone-receptor expression and ovarian cancer survival: an Ovarian Tumor Tissue Analysis consortium study. The Lancet Oncology. 2013; 14(9):853–62. [PubMed: 23845225]
17. Chan KK, Leung TH, Chan DW, Wei N, Lau GT, Liu SS, et al. Targeting estrogen receptor subtypes (ERalpha and ERbeta) with selective ER modulators in ovarian cancer. The Journal of endocrinology. 2014; 221(2):325–36. [PubMed: 24819599]
18. Murdoch WJ, Van Kirk EA, Isaak DD, Shen Y. Progesterone facilitates cisplatin toxicity in epithelial ovarian cancer cells and xenografts. Gynecologic oncology. 2008; 110(2):251–5. [PubMed: 18495224]
19. Fan HY, Liu Z, Paquet M, Wang J, Lydon JP, DeMayo FJ, et al. Cell type-specific targeted mutations of Kras and Pten document proliferation arrest in granulosa cells versus oncogenic insult to ovarian surface epithelial cells. Cancer research. 2009; 69(16):6463–72. [PubMed: 19679546]
20. Mullany LK, Fan HY, Liu Z, White LD, Marshall A, Gunaratne P, et al. Molecular and functional characteristics of ovarian surface epithelial cells transformed by KrasG12D and loss of Pten in a mouse model in vivo. Oncogene. 2011; 30(32):3522–36. [PubMed: 21423204]
21. Mullany LK, Liu Z, King ER, Wong KK, Richards JS. Wild-type tumor repressor protein 53 (Trp53) promotes ovarian cancer cell survival. Endocrinology. 2012; 153(4):1638–48. [PubMed: 22396451]
22. Lang GA, Iwakuma T, Suh YA, Liu G, Rao VA, Parant JM, et al. Gain of function of a p53 hot spot mutation in a mouse model of Li-Fraumeni syndrome. Cell. 2004; 119(6):861–72. [PubMed: 15607981]
23. Crane EK, Kwan SY, Izaguirre DI, Tsang YT, Mullany LK, Zu Z, et al. Nutlin-3a: A Potential Therapeutic Opportunity for TP53 Wild-Type Ovarian Carcinomas. PloS one. 2015; 10(8):e0135101. [PubMed: 26248031]
24. Liu S, Han SJ, Smith CL. Cooperative activation of gene expression by agonists and antagonists mediated by estrogen receptor heteroligand dimer complexes. Molecular pharmacology. 2013; 83(5):1066–77. [PubMed: 23462505]
25. Matsuo K, Nishimura M, Bottsford-Miller JN, Huang J, Komurov K, Armaiz-Pena GN, et al. Targeting SRC in mucinous ovarian carcinoma. Clin Cancer Res. 2011; 17(16):5367–78. [PubMed: 21737505]

26. Liu T, Hu W, Dalton HJ, Choi HJ, Huang J, Kang Y, et al. Targeting SRC and tubulin in mucinous ovarian carcinoma. Clin Cancer Res. 2013; 19(23):6532–43. [PubMed: 24100628]
27. Wang J, El-Bahrawy M. Expression profile of mucins (MUC1, MUC2, MUC5AC, and MUC6) in ovarian mucinous tumours: changes in expression from benign to malignant tumours. Histopathology. 2014
28. Cheng W, Liu J, Yoshida H, Rosen D, Naora H. Lineage infidelity of epithelial ovarian cancers is controlled by HOX genes that specify regional identity in the reproductive tract. Nature medicine. 2005; 11(5):531–7.
29. Mork L, Maatouk DM, McMahon JA, Guo JJ, Zhang P, McMahon AP, et al. Temporal differences in granulosa cell specification in the ovary reflect distinct follicle fates in mice. Biology of reproduction. 2012; 86(2):37. [PubMed: 21976597]
30. Perets R, Wyant GA, Muto KW, Bijron JG, Poole BB, Chin KT, et al. Transformation of the fallopian tube secretory epithelium leads to high-grade serous ovarian cancer in Brca;Tp53;Pten models. Cancer cell. 2013; 24(6):751–65. [PubMed: 24332043]
31. Rechsteiner M, Zimmermann AK, Wild PJ, Caduff R, von Teichman A, Fink D, et al. TP53 mutations are common in all subtypes of epithelial ovarian cancer and occur concomitantly with KRAS mutations in the mucinous type. Experimental and molecular pathology. 2013; 95(2):235–41. [PubMed: 23965232]
32. Shan W, Mercado-Uribe I, Zhang J, Rosen D, Zhang S, Wei J, et al. Mucinous adenocarcinoma developed from human fallopian tube epithelial cells through defined genetic modifications. Cell Cycle. 2012; 11(11):2107–13. [PubMed: 22592533]
33. Rasti M, Arabsolghar R, Khatooni Z, Mostafavi-Pour Z. p53 Binds to estrogen receptor 1 promoter in human breast cancer cells. Pathology oncology research : POR. 2012; 18(2):169–75. [PubMed: 21655924]
34. Shirley SH, Rundhaug JE, Tian J, Cullinan-Ammann N, Lambertz I, Conti CJ, et al. Transcriptional regulation of estrogen receptor-alpha by p53 in human breast cancer cells. Cancer research. 2009; 69(8):3405–14. [PubMed: 19351845]
35. Junk DJ, Vrba L, Watts GS, Oshiro MM, Martinez JD, Futscher BW. Different Mutant/Wild-Type p53 Combinations Cause a Spectrum of Increased Invasive Potential in Nonmalignant Immortalized Human Mammary Epithelial Cells. Neoplasia. 2008; 10(5):450–61. [PubMed: 18472962]
36. Brown J, Frumovitz M. Mucinous tumors of the ovary: current thoughts on diagnosis and management. Current oncology reports. 2014; 16(6):389. [PubMed: 24777667]
37. Vassilev LT, Vu BT, Graves B, Carvajal D, Podlaski F, Filipovic Z, et al. In vivo activation of the p53 pathway by small-molecule antagonists of MDM2. Science. 2004; 303(5659):844–8. [PubMed: 14704432]
38. Tovar C, Rosinski J, Filipovic Z, Higgins B, Kolinsky K, Hilton H, et al. Small-molecule MDM2 antagonists reveal aberrant p53 signaling in cancer: implications for therapy. Proceedings of the National Academy of Sciences of the United States of America. 2006; 103(6):1888–93. [PubMed: 16443686]
39. Kenny HA, Chiang CY, White EA, Schryver EM, Habis M, Romero IL, et al. Mesothelial cells promote early ovarian cancer metastasis through fibronectin secretion. The Journal of clinical investigation. 2014; 124(10):4614–28. [PubMed: 25202979]
40. Ledermann JA, Luvero D, Shafer A, O'Connor D, Mangili G, Friedlander M, et al. Gynecologic Cancer InterGroup (GCIG) consensus review for mucinous ovarian carcinoma. International journal of gynecological cancer : official journal of the International Gynecological Cancer Society. 2014; 24(9 Suppl 3):S14–9. [PubMed: 25341574]
41. Gemignani ML, Schlaerth AC, Bogomolniy F, Barakat RR, Lin O, Soslow R, et al. Role of KRAS and BRAF gene mutations in mucinous ovarian carcinoma. Gynecologic oncology. 2003; 90(2): 378–81. [PubMed: 12893203]
42. Mayr D, Hirschmann A, Lohrs U, Diebold J. KRAS and BRAF mutations in ovarian tumors: a comprehensive study of invasive carcinomas, borderline tumors and extraovarian implants. Gynecologic oncology. 2006; 103(3):883–7. [PubMed: 16806438]

43. Auner V, Kriegshauser G, Tong D, Horvat R, Reinthaller A, Mustea A, et al. KRAS mutation analysis in ovarian samples using a high sensitivity biochip assay. BMC cancer. 2009; 9:111. [PubMed: 19358724]
44. Silva JL, De Moura Gallo CV, Costa DC, Rangel LP. Prion-like aggregation of mutant p53 in cancer. Trends in biochemical sciences. 2014; 39(6):260–7. [PubMed: 24775734]
45. Willis A, Jung EJ, Wakefield T, Chen X. Mutant p53 exerts a dominant negative effect by preventing wild-type p53 from binding to the promoter of its target genes. Oncogene. 2004; 23(13):2330–8. [PubMed: 14743206]
46. Wang Y, Suh YA, Fuller MY, Jackson JG, Xiong S, Terzian T, et al. Restoring expression of wild-type p53 suppresses tumor growth but does not cause tumor regression in mice with a p53 missense mutation. The Journal of clinical investigation. 2011; 121(3):893–904. [PubMed: 21285512]
47. Miller SJ, Lan ZD, Hardiman A, Wu J, Kordich JJ, Patmore DM, et al. Inhibition of Eyes Absent Homolog 4 expression induces malignant peripheral nerve sheath tumor necrosis. Oncogene. 2010; 29(3):368–79. [PubMed: 19901965]
48. Depreux FF, Darrow K, Conner DA, Eavey RD, Liberman MC, Seidman CE, et al. Eya4-deficient mice are a model for heritable otitis media. The Journal of clinical investigation. 2008; 118(2): 651–8. [PubMed: 18219393]
49. Li H, Diao TY, Zhou ZY, Yang FY, Ma Q, Li QH. Relationship between the expression of hTERT and EYA4 mRNA in peripheral blood mononuclear cells with the progressive stages of carcinogenesis of the esophagus. Journal of experimental & clinical cancer research : CR. 2009; 28:145. [PubMed: 19939248]
50. Tadjuidje E, Hegde RS. The Eyes Absent proteins in development and disease. Cellular and molecular life sciences : CMLS. 2013; 70(11):1897–913. [PubMed: 22971774]

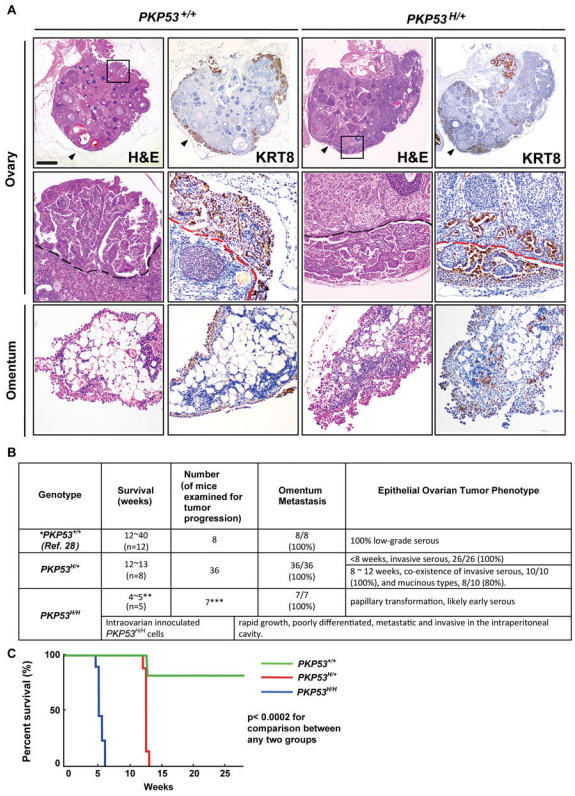

Figure 1.

Mutant *Trp53*^{R172H} allele promotes epithelial ovarian tumor progression. A, Representative images of tissue sections stained with H&E or KRT8 of ovaries and omentum from *PKP53*$^{+/+}$ and *PKP53*$^{H/+}$ mice at 12 weeks of age. Regions in frame are shown at higher magnification below. Black and red dashed lines: the surface of the ovary. Black arrow heads: ovarian bursa. Scale bar: 400 μm (top row) and 80 μm (bottom two rows). B, Survival ages and phenotypic characteristics of mutant mice with different p53 status. *Data presented here on *PKP53*$^{+/+}$ mice are from previous published studies and new information collected from the current study (19). ** *PKP53*$^{H/H}$ mice die rapidly from unknown causes. ***Female progenies with homozygous *Trp53*$^{R172H/R172H}$ mutation are born at lower than Mendelian ratio due to female-specific exencephaly, thus making it harder to obtain large sample size for the cohort. C, Kaplan-Meier analysis shows that *Trp53*$^{R172H/R172H}$ homozygous mutation is associated with the shortest term of survival, and *Trp53*$^{R172H/+}$ heterozygous mutation is associated with significantly reduced term of survival compared to mice expressing wild type *Trp53*. ($p<0.0002$ for comparison between any two groups, log-rank test).

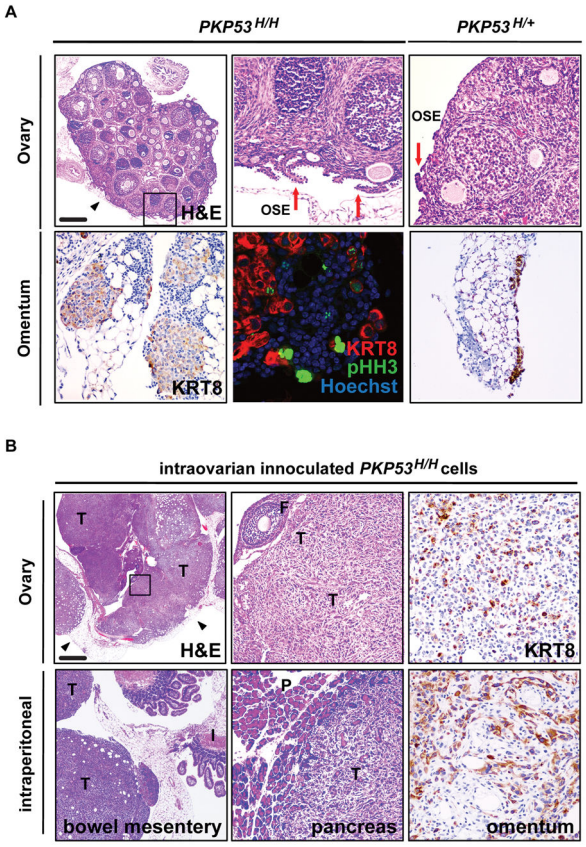

Figure 2.

Epithelial ovarian tumors expressing homozygous *Trp53*^{R172H} mutation have early onset and metastasis. A, Representative images of tissue sections stained with H&E, KRT8, or KRT8 and pHH3 on ovaries (top panels) or omentum (bottom panel) from *PKP53*$^{H/H}$ and *PKP53*$^{H/+}$ mice at 4 weeks of age. Regions in frames are shown at higher magnification at the right. Scale bar: 400 μm, 80 μm, and 40 μm. B, Representative images of H&E and KRT8 staining on sections of tumors from intraovarian innoculated *PKP53*$^{H/H}$ cells. Region in frame is shown at higher magnification at the right. F=follicle; T=tumor; I=intestine; P=pancreas. Scale bar: 750 μm, 200 μm, 100 μm and 50 μm.

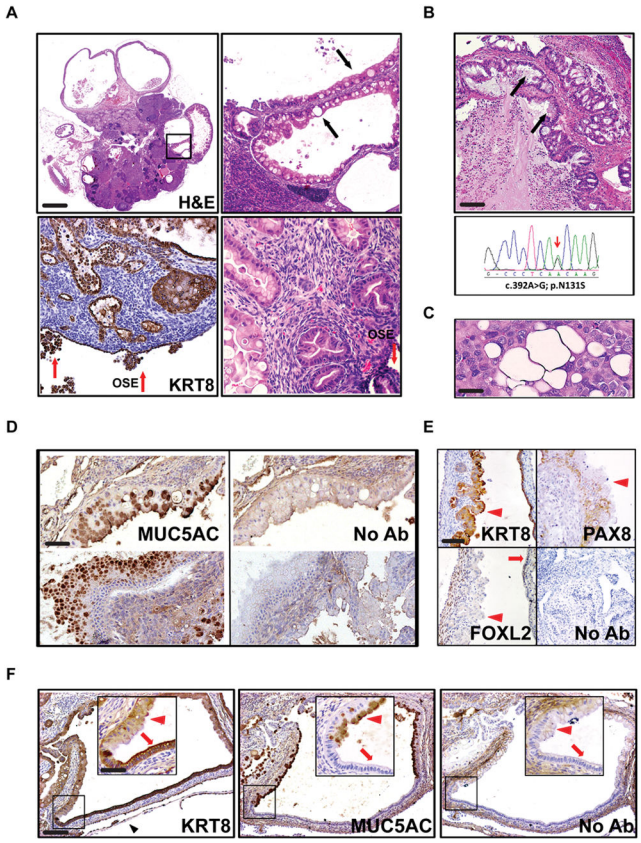

Figure 3.

Mucinous epithelial ovarian tumors develop in *PKP53*$^{H/+}$ mice. A, At 12 weeks of age, 80% of *PKP53*$^{H/+}$ mice develop mucinous structures and some of them become cystic (top panel). Regions in frame are shown at higher magnification at the right. Red arrows: OSE cells. Black arrows: secretory mucinous structures. Scale bar: 900μm, 180 μm and 90 μm. B, Representative image of H&E stained human mucinous EOC tumor (upper panel) and the corresponding sequencing results of the TP53 gene in laser capture microdissected tumor cells from the same patient. Black arrows: secretory mucinous structures. Scale bar: 200 μm. C, The RMUG-L human cell line, derived from a mucinous ovarian carcinoma, carries heterozygous WT and mutant *TP53* alleles and exhibits secretory mucinous structures when innoculated into the intraperitoneal cavity of SCID mice. Scale bar: 25 μm. D, Mucinous structures in *PKP53*$^{H/+}$ mice express MUC5AC, a marker for human mucinous ovarian carcinoma. Adjacent sections without first antibody were used as negative controls. Scale bar: 100 μm. E, Mucinous structures in *PKP53*$^{H/+}$ mice express KRT8 but do not express FOXL2 (nuclear staining) or PAX8 (nuclear staining). Red arrowheads: mucinous structures; red arrows: epithelial structures. Scale bar: 150 μm. F, Some cystic structures in the ovary of *PKP53*$^{H/+}$ mice contain contiguous regions that are positive for both MUC5AC and KRT8 (red arrow heads) or for KRT8 alone (red arrows) (inserts are higher magnification of regions in frames). Black arrowhead: ovarian bursa. Scale bar: 200 μm and 100 μm.

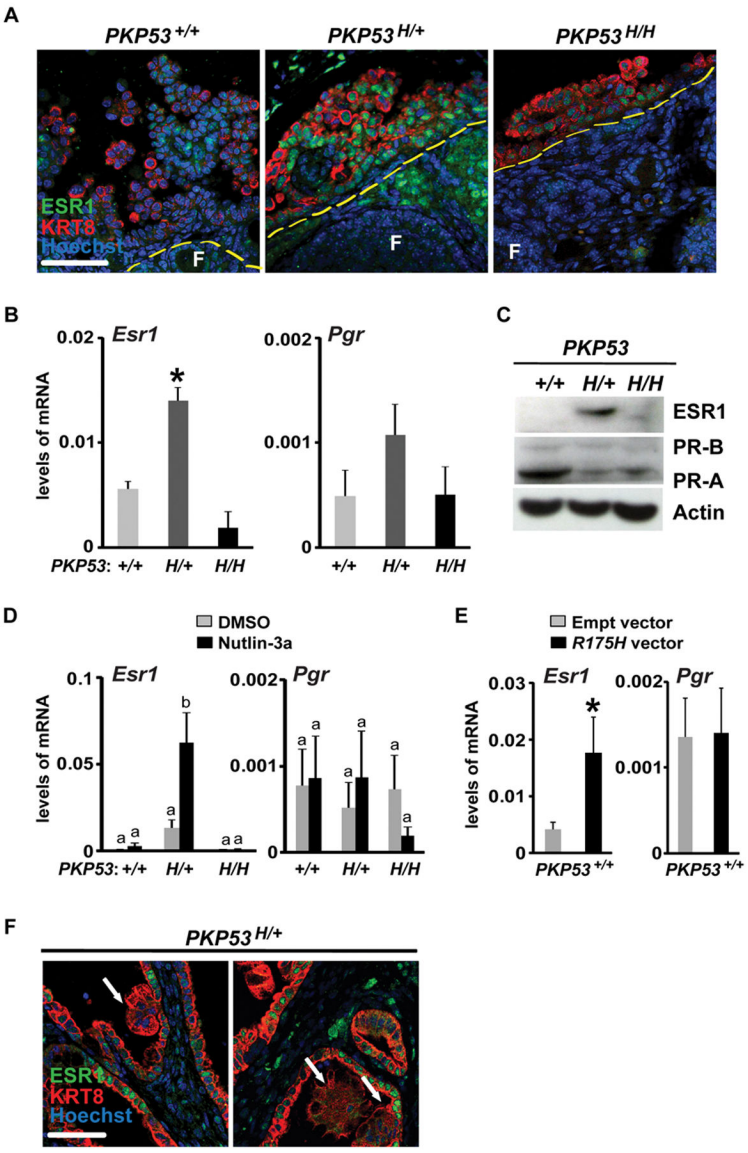

Figure 4.

Expression of ESR1 is elevated in OSE cells of *PKP53*$^{H/+}$ mice. A, Representative images of immunofluorescent staining of ESR1 and KRT8 in OSE cells of ovarian tissue sections. Yellow dash lines: the surface of the ovary. F=follicles. Scale bar: 50 μm. B, Levels of *Esr1* and *Pgr* mRNA in isolated and un-passaged OSE cells quantified by RT-PCR and normalized to *Rpl19* expression. Data are represented as mean ± SEM (n=5 mice per genotype). *p<0.05. C, Representative images of Western blot for ESR1, PR-A, PR-B and beta-Actin in OSE cell lines. D, Levels of *Esr1* and *Pgr* mRNA in OSE cells treated with DMSO or nutlin-3a (10 μM) and quantified by RT-PCR and normalized to *Rpl19* expression. Data are represented as mean ± SEM (n=3 different experimental replicates). Bars without common superscript are significantly different, *p<0.05. E, Levels of *Esr1* and *Pgr* mRNA in *PKP53*$^{+/+}$ OSE cells expressing empty vector or vector expressing the R172H mutant allele,

and quantified by RT-PCR and normalized to *Rpl19* expression. Data are represented as mean ± SEM (n=3 different experimental replicates). *p<0.05.

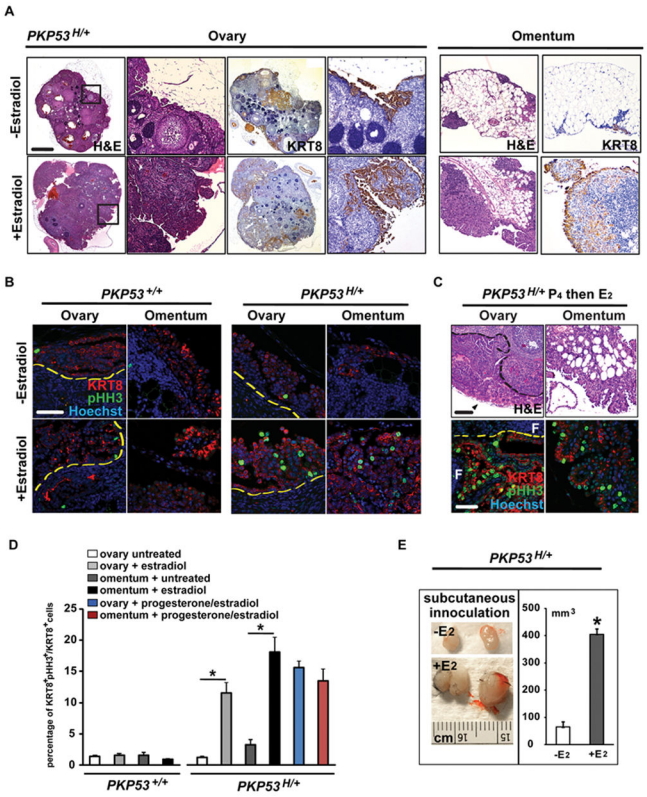

Figure 5.

Estradiol promotes tumor growth on the ovary and omentum in *PKP53*$^{H/+}$ Mice. A, Representative images of H&E and KRT8 staining of ovarian tissue sections from *PKP53*$^{H/+}$ mice. Regions in frames are shown at higher power at the right. Scale bar: 750 μm and 150 μm. B, Immunofluorescent staining of pHH3 and KRT8 on sections of ovaries and omentum from *PKP53*$^{+/+}$ and *PKP53*$^{H/+}$ mice with or without *in vivo* estradiol treatment. Yellow dashed lines: the surface of the ovary. C, Representative images of H&E and KRT8 and pHH3 staining of ovarian tissue sections from *PKP53*$^{H/+}$ mice implanted with progesterone pellets one day before estradiol pellets. Black arrowheads: transformed OSE cells. Dashed lines: the surface of the ovary. F: follicles. Scale bar: 100 and 50 μm. D, Quantification of the percentage of KRT8^{+}pHH3^{+} cells among KRT8^{+} cells with visible nuclei was performed on representative images taken from different mice of each genotype (n=4). Data are represented as mean ± SEM. *p<0.05. Scale bar: 50 μm. E, Estradiol promotes the growth of subcutaneously injected *PKP53*$^{H/+}$ OSE cells into syngenic mice (n=5). *p<0.01. D, Primary tumors on the ovary (top panels) and metastatic tumors on the omentum (bottom panel) showed extensive growth when the progesterone pellet was implanted one day before the estradiol pellet. Black arrowheads: ovarian bursa. Dashed lines: the surface of the ovary.

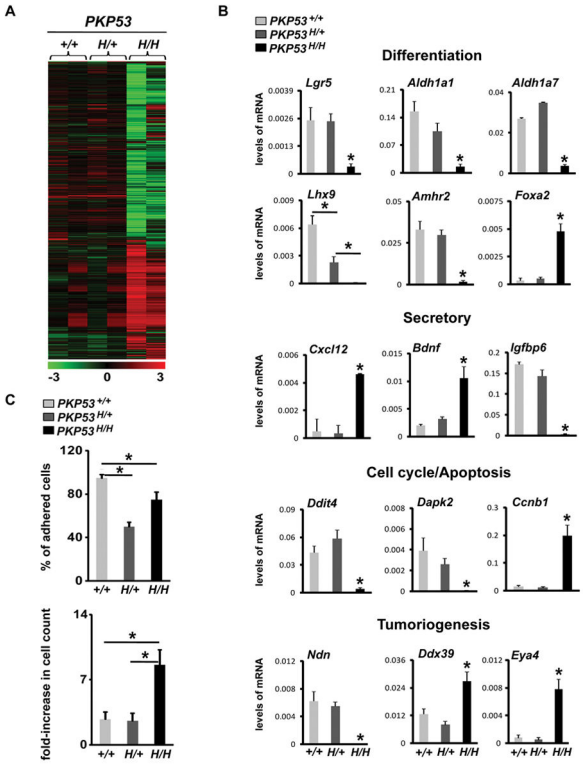

Figure 6.

Expression of the *Trp53*^{R172H} mutant allele alters OSE tumor differentiation and promotes their proliferation and survival. A, Heatmap comparison of gene expression profiles from microarray analyses of OSE cells isolated from *PKP53*$^{+/+}$, *PKP53*$^{H/+}$ and *PKP53*$^{H/H}$ mice. B, RT-PCR quantification and verification of selected genes in functional categories with different levels according to the microarray analyses. Data are represented as mean ± SEM (n=5). *p<0.05. C, Expression of the *Trp53*^{R172H} mutant allele alters OSE cell adhesion (top panel) and proliferation (bottom panel) in culture. This experiment was repeated 3 times and each experiment contains 4 replicates for each genotype. Data are represented as mean ± SEM. *p<0.01.

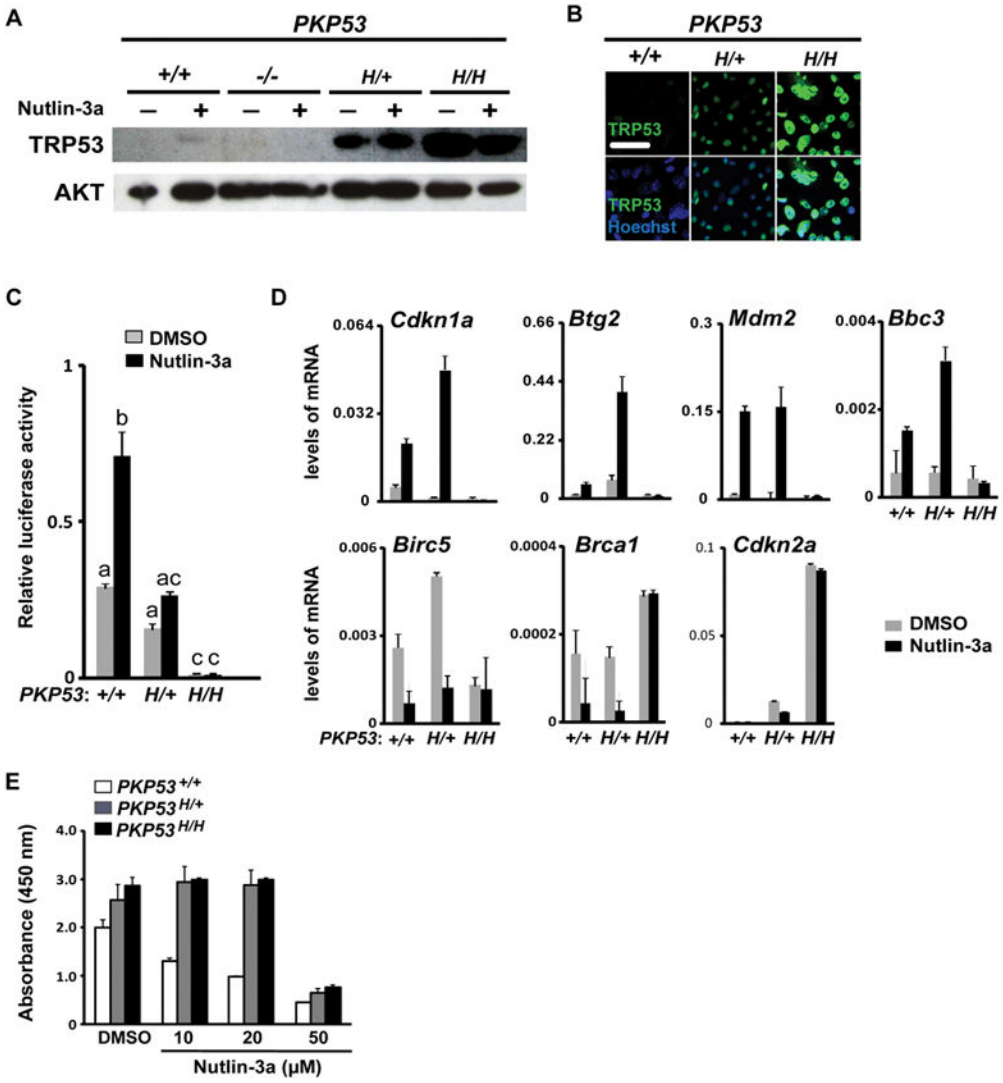

Figure 7.

Mutant *Trp53*^{R172H} alters TRP53 activity in OSE tumors. A, Representative Western blot analyses of TRP53 and AKT in OSE cells of different genotypes treated with DMSO or nutlin-3a (10 μM). B, Representative immunofluorescent staining of TRP53 in cultured OSE cells. Scale bar: 25 μm. C, Relative luciferase activity of a p53 reporter construct. Data is representative of experiments repeated 4 times and in each experiment luciferase activity was measured in triplicates. Bars without common superscript are significantly different, *p<0.05. D, Expression of the *Trp53*^{R172H} mutant allele alters mRNA levels of both TRP53-induced (upper panels) and -suppressed genes (lower panels) in response to nutlin-3a treatment (n=3). E, Cell viability in response to nutlin-3a treatment (72 hr) as measured by the WST-1 assay. This experiment was repeated 3 times and each experiment contains 3 replicates for each genotype. Data are represented as mean ± SEM.